Acetabular Cartilage Assessment in Patients with Femoroacetabular Impingement by Using T2* Mapping with Arthroscopic Verification[1]

Jutta Ellermann, MD, PhD
Connor Ziegler, MD
Mikko J. Nissi, PhD
Rainer Goebel, PhD
John Hughes, PhD
Michael Benson, BS
Peter Holmberg, BS
Patrick Morgan, MD

Purpose: To evaluate the ability of T2* mapping to help differentiate damaged from normal acetabular cartilage in patients with femoroacetabular impingement (FAI).

Materials and Methods: The institutional review board approved this retrospective study, and the requirement to obtain informed consent was waived. The study complied with HIPAA guidelines. The authors reviewed T2* relaxation time maps of 28 hips from 26 consecutive patients (mean patient age, 28.2 years; range, 12–53 years; eight male patients (nine hips) with a mean age of 26.7 years [range, 16–53 years]; 18 female patients (19 hips) with a mean age of 28.9 years [range, 12–46 years]). Conventional diagnostic 3.0-T magnetic resonance (MR) arthrography was augmented by including a multiecho gradient-recalled echo sequence for T2* mapping. After imaging, acetabular and femoral data were separated and acetabular regions of interest were identified. Arthroscopic cartilage assessment with use of a modified Beck scale for acetabular cartilage damage was performed by an orthopedic surgeon who was blinded to the results of T2* mapping. A patient-specific acetabular projection with a T2* overlay was developed to anatomically correlate imaging data with those from surgery (the standard of reference). Results were analyzed by using receiver operating characteristic (ROC) curves.

Results: The patient-specific acetabular projection enabled colocalization between the MR imaging and arthroscopic findings. T2* relaxation times for normal cartilage (Beck score 1, 35.3 msec ± 7.0) were significantly higher than those for cartilage with early changes (Beck score 2, 20.7 msec ± 6.0) and cartilage with more advanced degeneration (Beck scores 3–6, ≤19.8 msec ± 5.6) ($P < .001$). At ROC curve analysis, a T2* value of 28 msec was identified as the threshold for damaged cartilage, with a 91% true-positive and 13% false-positive rate for differentiating Beck score 1 cartilage (normal) from all other cartilages.

Conclusion: The patient-specific acetabular projection with a T2* mapping overlay enabled good anatomic localization of cartilage damage defined with a T2* threshold of 28 msec and less.

[1] From the Center for Magnetic Resonance Research, Department of Radiology (J.E., C.Z., M.J.N., M.B., P.H.), Department of Orthopaedic Surgery (M.J.N., M.B., P.M.), and Division of Biostatistics, School of Public Health (J.H.), University of Minnesota, 2021 6th St SE, 2-130 CMRR Building, Minneapolis, MN 55455; and Department of Psychology and Neuroscience, Maastricht University, Maastricht, the Netherlands (R.G.). From the 2011 RSNA Annual Meeting. Received August 21, 2013; revision requested September 27; revision received October 25; accepted November 12; final version accepted November 22. **Address correspondence to** J.E. (e-mail: *eller001@umn.edu*).

Femoroacetabular impingement (FAI) is a common cause of hip pain and is due to abnormal periarticular morphology that results in pathologic abutment between the head-neck junction and the acetabular rim (1,2). FAI has been shown to cause labral and chondral lesions and lead to osteoarthritis (3–6). Joint preservation surgery is recommended for patients with symptoms unamenable to medical management who have normal or limited cartilage damage (7–9). Joint preservation procedures are contraindicated in patients with moderate to advanced cartilage changes because these levels of cartilage abnormality are associated with early failure and conversion to total hip arthroplasty (10,11). Moderate cartilage damage, unfortunately, can be a challenge to diagnose (12). Radiographic evaluation with use of Tönnis grading is the standard of care but has been shown to have poor interobserver reliability (13–15). Magnetic resonance (MR) imaging evaluation would seem to be the logical alternative. The accuracy of MR imaging and MR arthrography for detecting chondral damage in FAI, however, is poor (12,16–20). The identification of cartilage damage in FAI may be difficult owing to the pattern of cartilage damage particular to this condition (21).

In FAI, cartilage damage is frequently limited to the acetabulum and occurs deep within the tissue as a debonding of articular cartilage from bone (3). This leaves the superficial layer intact, a pattern uniquely ill-suited for diagnosis with traditional MR imaging—which is best at depicting a void at the articular surface. As a consequence, investigators have turned to quantitative MR mapping techniques such as delayed gadolinium-enhanced MR imaging of cartilage (22–25) and T2 mapping (26–29). Delayed gadolinium-enhanced MR imaging of cartilage is the most widely applied investigational technique. It can, however, be time-consuming and logistically difficult to perform and currently gives a combined value for femoral and acetabular cartilage (30). T2 relaxation time measurements (26–29) and, more recently, T2* mapping have been reported in the hip (31–34). We speculated as to whether T2* mapping had the potential to be clinically practical for routine cartilage assessment because it takes little time, does not require contrast material, and is able to help differentiate femoral from acetabular cartilage.

The purpose of our study, therefore, was to evaluate the ability of T2* mapping to help differentiate damaged from normal articular cartilage in patients with FAI. To do so, we sought to develop an anatomically precise technique with which to visualize T2* data; to then use this visualization method to compare T2* data with a surgical standard of reference; and, if successful, to use a receiver operating characteristic (ROC) curve to define a threshold T2* value for damaged acetabular cartilage, which would increase our ability to interpret T2* values in the future.

Advances in Knowledge

- In patients with femoroacetabular impingement, T2* maps were found to have significantly lower values in regions with surgically identified cartilage damage (mean, 20.7 msec ± 6.0) than in normal cartilage (mean, 35.3 msec ± 7.0) ($P < .001$).
- A patient-specific acetabular projection with a T2* mapping overlay was developed to anatomically correlate imaging data with those from arthroscopy (the standard of reference) on the basis of the Beck scale for cartilage damage.
- Receiver operating characteristic curve analysis was used to define a threshold T2* value for damaged acetabular cartilage as 28 msec and less.
- Despite the elimination of surgical candidates with joint space narrowing or increased sclerosis, patients with Tönnis grade 1 were found at surgery to have cartilage damage in 360 of the 532 regions of interest (68%) and no hyaline cartilage in 29 (5%); this underscores the insensitivity of radiographs in determining the extent of osteoarthritis in this cohort.

Implications for Patient Care

- T2* mapping may become a valuable method for the routine evaluation of articular cartilage with clinical MR units because it requires little additional time and no intravenous or intraarticular contrast material.
- A patient-specific acetabular projection enables good anatomic localization of MR data and facilitates both preoperative patient assessment and the monitoring of specific cartilage lesions over time.
- The T2* threshold for articular cartilage damage, with use of the defined protocol at 3.0 T, increases our ability to interpret T2* values.

Materials and Methods

Patients and Clinical Assessment

The institutional review board approved this retrospective study, and the requirement to obtain informed

Published online before print
10.1148/radiol.13131837 **Content codes:** MK

Radiology 2014; 271:512–523

Abbreviations:
FAI = femoroacetabular impingement
ROC = receiver operating characteristic
ROI = region of interest
3D = three-dimensional

Author contributions:
Guarantors of integrity of entire study, J.E., C.Z., P.M.; study concepts/study design or data acquisition or data analysis/interpretation, all authors; manuscript drafting or manuscript revision for important intellectual content, all authors; manuscript final version approval, all authors; literature research, J.E., C.Z., M.J.N., P.H., P.M.; clinical studies, J.E., C.Z., P.H., P.M.; statistical analysis, J.E., C.Z., M.J.N., R.G., J.H., M.B.; and manuscript editing, all authors

Conflicts of interest are listed at the end of this article.

Table 1

Imaging Parameters for MR Arthrography

Sequence*	Plane	TR/TE (msec)†	No. of Sections	Section Thickness (mm)	Resolution (mm)	Imaging Time
T1-weighted TSE FS	Axial, sagittal, coronal	540–780/10–12	24	3–4	0.45 × 0.6	3–4 min
T2-weighted TSE FS	Coronal, sagittal	2200–2600/68–75	24	3–4	0.45 × 0.6	3–4 min
PD-weighted TSE	Coronal, oblique, axial	2000–2200/27–39	24	3–4	0.45 × 0.6	3–4 min
SPACE	3D	1000/30	…	…	0.75 × 0.75 × 0.75	5 min 17 sec
DESS	3D	12/4.9	…	…	0.75 × 0.75 × 0.75 or 1 × 1 × 1	5 min 50 sec
T2*-weighted GRE FS	Sagittal	1040/4.2, 11.3, 18.4, 25.6, 32.7	24	3	0.52 × 0.52 interpolated to 0.26 × 0.26	7 min

Note.—MR arthrography was performed after the administration of a dilute solution (2.5 mmol/L) of gadopentetate dimeglumine (Magnevist; Berlex Laboratories, Wayne, NJ).

* DESS = double-echo steady state, FS = fat saturated, GRE = gradient-recalled echo, PD = proton density, SPACE = sampling perfection with application optimized contrasts using different flip angle evolutions (three-dimensional [3D] turbo spin echo with variable flip angle), TSE = turbo spin echo.

† TR/TE = repetition time/echo time.

consent was waived. Compliance with the Health Insurance Portability and Accountability Act was maintained throughout.

All hip MR images obtained between February 2010 and March 2012 were retrospectively assessed. Included were all consecutive patients with the clinical diagnosis and radiographic signs of FAI without evidence of osteoarthritis who underwent the study imaging protocol, who were diagnosed with a labral tear, and who subsequently underwent hip arthroscopy after conservative treatment failed. The clinical diagnosis of FAI was established by the presence of *(a)* moderate-to-severe persistent hip or groin pain that limited activity and worsened with flexion activity and *(b)* positive impingement sign (sudden pain at 90° hip flexion with adduction and internal rotation or extension and external rotation). Radiographic confirmation of FAI included findings such as α angle greater than 50°, pistol grip deformity, coxa profunda, and/or acetabular retroversion. Exclusion criteria were osteoarthritis as evidenced by radiographic changes (Tönnis grade >1) (15), previous hip surgery, or diagnosis of other abnormalities to explain the hip pain. All patients were examined by the same orthopedic surgeon, who specialized in hip arthroscopy (P.M., with 7 years of experience), and evaluated with standardized radiographs per published protocol (35).

MR Imaging and Image Processing

A 3.0-T clinical imaging protocol (Trio; Siemens Medical Solutions, Erlangen, Germany) and a body matrix phased-array coil were used. This protocol is detailed in Table 1. A representative set of images from clinical MR arthrography is shown in Figure 1. The protocol required approximately 45 minutes to complete, with the T2* data obtained during the final 7 minutes to prevent time dependence of T2* values after unloading (34). T2* maps were generated inline by using software (Mapit; Siemens Medical Solutions).

Postprocessing was performed independently by the primary reviewer (C.Z., a 2nd year orthopedic resident), who was blinded to the patients' clinical information. Acetabular orientation was standardized on sagittal images by using a line passing through the center of the femoral head, perpendicular to the transverse acetabular ligament defining the 12-o'clock position superiorly and the 3-o'clock position anteriorly (Fig 2). The border between the acetabular and femoral articular cartilage layers was defined as the low-signal-intensity line (Fig 2) seen on the second echo of the gradient-recalled echo sequence (echo time = 11.2 msec). Cartilage damage ROIs were defined in the anterosuperior acetabulum because this area has the highest reported incidence of damage in patients with FAI (3,16,36). Acetabular cartilage in this region as seen on three consecutive sagittal sections was divided into five ROIs in each section between the 12-o'clock position and the chondrolabral junction (Fig 2) by using the image processing application OsiriX (OsiriX v.4.1.1; 32 bit, *http://www.osirix-viewer.com/*) (37), for a total of 15 anterosuperior ROIs. For the assessment of differences between deep and superficial tissue layers, each ROI was further split in half depth-wise. Each layer plus the full-thickness acetabular cartilage was subsequently assessed. Four ROIs were defined in the posteromedial acetabulum, where articular cartilage damage is infrequent in FAI, to serve as control ROIs. These were processed in an identical fashion. Note that this landmark-based definition resulted in ROIs comparable between the patients even though the volume (and number of voxels) varied from patient to patient depending on their physical size. To enable comparison with surgical assessment, imaging data were anatomically located to their position on the patient's acetabulum with use of a patient-specific, flattened acetabular projection. Flattened projections were created by first segmenting the acetabular cartilage with data from either 3D double-echo steady-state or 3D

Figure 1

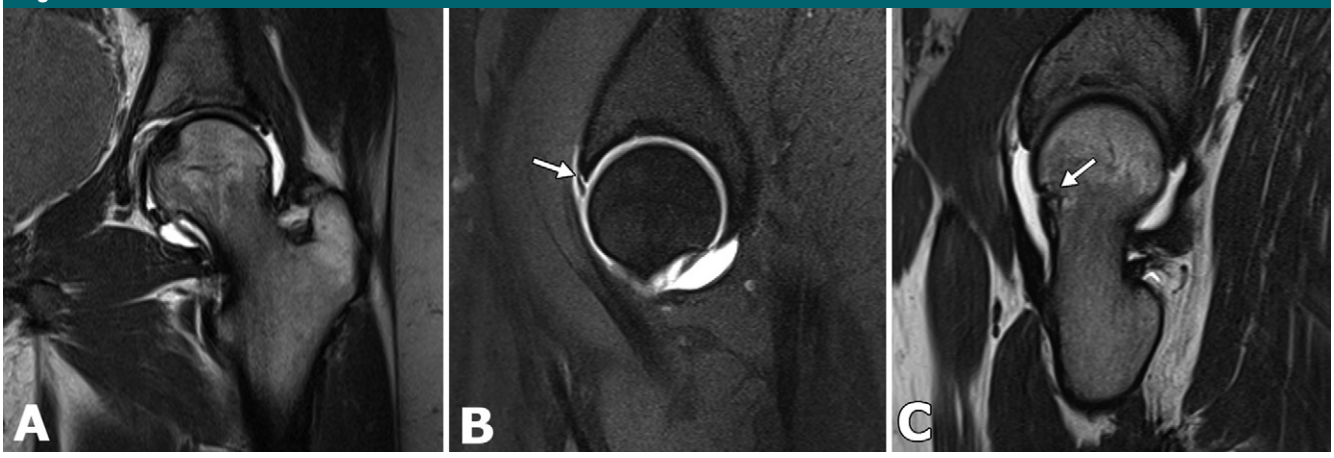

Figure 1: Images from MR arthrography of right hip. *A*, Coronal proton density–weighted, *B*, sagittal fat-suppressed T1-weighted (repetition time msec/echo time msec = 780/12, 3-mm-thick sections), and, *C*, axial oblique proton density–weighted (2200/37, 3-mm-thick sections) images. Coronal image depicts preserved joint space, with no definite evidence of cartilage damage. Sagittal image reveals high-signal-intensity contrast material interposed at chondrolabral junction, a finding that is most consistent with labral tear (arrow). Arrow on axial oblique image indicates irregular-appearing reduced femoral head-neck offset (bump).

Figure 2

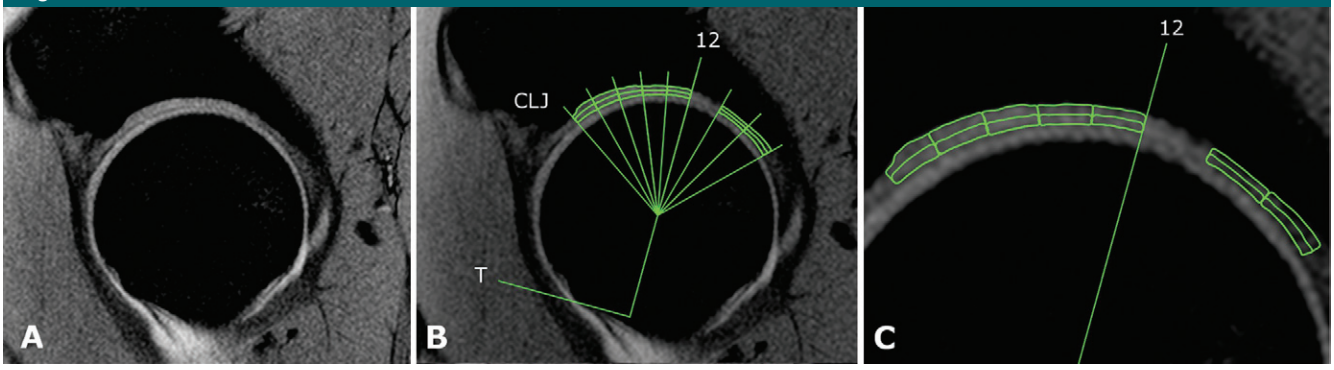

Figure 2: Selection of ROIs in acetabulum for statistical analysis of T2* data. *A*, T2* gradient-recalled echo image (echo time, 11.2 sec) shows acetabular and femoral articular cartilage layers separated at low-signal-intensity line interposed between two sides of joint. Acquired in-plane resolution was 0.52 × 0.52 mm, interpolated to 0.26 × 0.26 mm, which allowed for 3–6 voxels within acetabular cartilage only, depending on cartilage thickness. *B*, Sagittal view of hip shows guides for 12-o'clock line, angular guides for five selected ROIs in anterosuperior labrum between 12-o'clock position and chondrolabral junction (*CLJ*), and angular guides for two control ROIs at fixed 10:30–11:30 positions. Transverse ligament (*T*) was used as anatomic landmark to consistently derive 12-o'clock position as an orthogonal line through center of femoral head, assuming that 12-o'clock position is superior and 3-o'clock position is anterior. *C*, Magnified area shows five zones of superficial and deep ROIs in anterosuperior acetabular cartilage. Also shown are two control zones of superficial and deep ROIs at fixed 10:30–11:30 positions. Magnified portion better illustrates delineation of acetabular and femoral cartilage with a thin dark line interposed between the two.

turbo spin-echo with variable flip angle (SPACE, or sampling perfection with application optimized contrasts using different flip angle evolutions) imaging, depending on which was available in the clinical protocol. A 3D volume mesh was then generated from the segmentation data by using software (BrainVoyager QX 2.4, *http://www.brainvoyager.com/*) (38). T2* maps were coregistered with the anatomic data and then sampled on the surface of this 3D mesh by using BrainVoyager and Matlab (Matlab 2011b; MathWorks, Natick, Mass) to generate surface maps representing the T2* data of the acetabular cartilage. Finally, the 3D mesh of the acetabular cartilage was flattened on a two-dimensional plane by using BrainVoyager and the T2* surface map was then applied on the flattened mesh, allowing the entire anatomically located set of T2* acetabular data to be seen on a single image (Fig 3).

Arthroscopy

All arthroscopic examinations were performed by the same orthopedic surgeon (P.M., with 7 years of experience). The orthopedic surgeon was

Figure 3

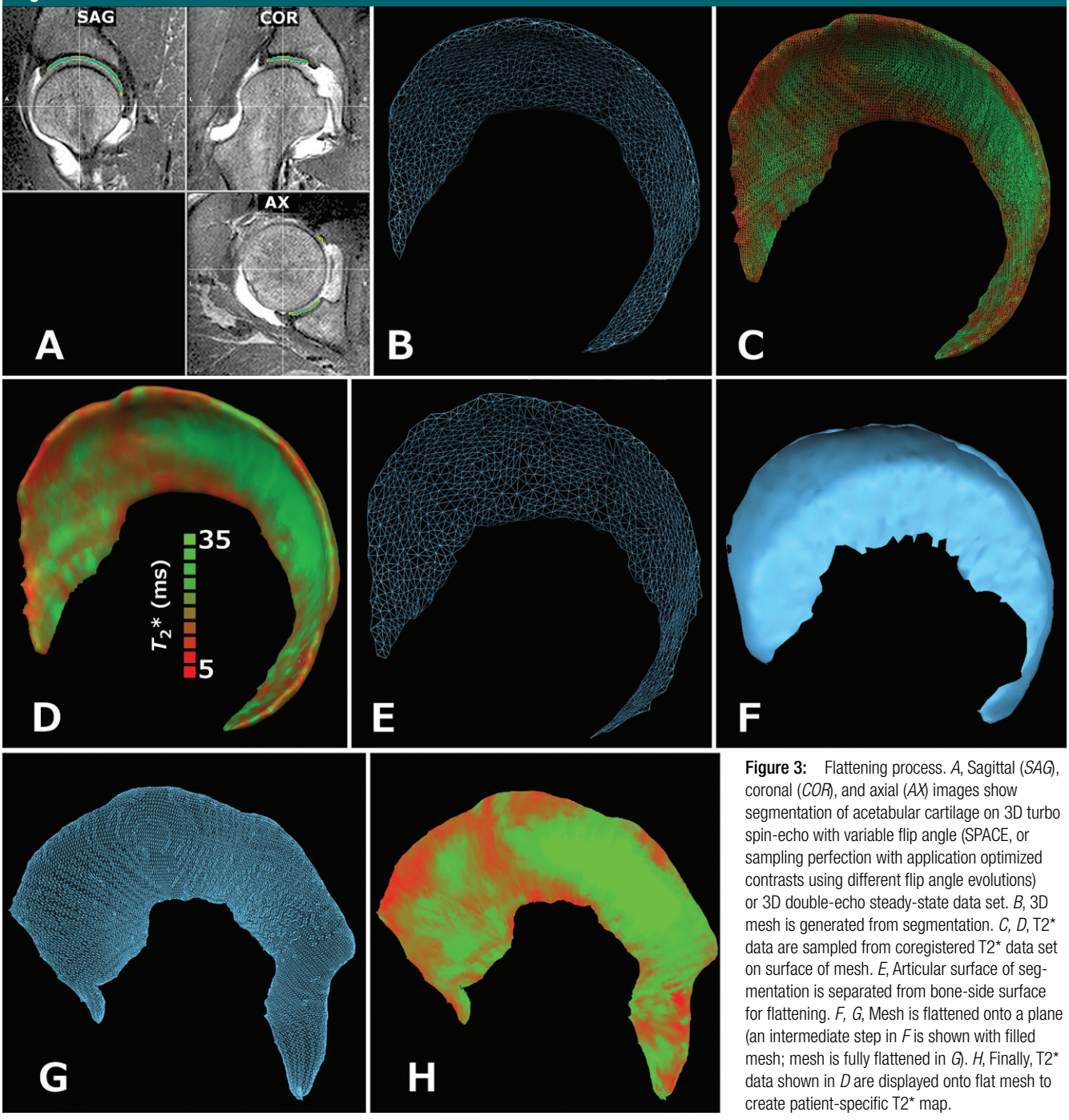

Figure 3: Flattening process. *A*, Sagittal (*SAG*), coronal (*COR*), and axial (*AX*) images show segmentation of acetabular cartilage on 3D turbo spin-echo with variable flip angle (SPACE, or sampling perfection with application optimized contrasts using different flip angle evolutions) or 3D double-echo steady-state data set. *B*, 3D mesh is generated from segmentation. *C, D*, T2* data are sampled from coregistered T2* data set on surface of mesh. *E*, Articular surface of segmentation is separated from bone-side surface for flattening. *F, G*, Mesh is flattened onto a plane (an intermediate step in *F* is shown with filled mesh; mesh is fully flattened in *G*). *H*, Finally, T2* data shown in *D* are displayed onto flat mesh to create patient-specific T2* map.

presented with a patient-individualized, flattened anatomic map of the acetabulum, on which simple, obvious bony landmarks could be located at surgery. The psoas sulcus, the highest point of the acetabular notch along with the parallel medial and lateral borders of the acetabular notch, and the base of the anterior lunate cartilage were readily used to define the midpoint, top, and bottom of the anterior lunate cartilage, respectively. The medial borders of the notch define the lunate's anteromedial borders. The posterior lunate has a consistent sulcus similar to the anterior

Table 2

Modified Beck Scale

Score	Description	Criteria
1	Normal	Macroscopically sound cartilage
2	Early changes	Softening, fibrillation, cartilage remains adherent to underlying bone
3	Debonding	Loss of fixation to the subchondral bone, carpet phenomenon
4	Cleavage	Loss of fixation to the subchondral bone, frayed edges, thinning of the cartilage, flap
5	Defect, fibrous base	Full-thickness loss of articular cartilage with a thin fibrous tissue–covered base
6	Defect, eburnated base	Full-thickness cartilage loss with a base of eburnated bone

psoas sulcus and the superior point of the notch. Individual ROIs, once located in space, were measured relative to a flexible probe measuring 2 mm in diameter, which served as a ruler. Because each patient had individualized ROIs known to the surgeon (who was blinded to the T2* values), the correlation between the patient-individualized anatomic maps and the arthroscopic findings was accomplished by locating the ROI by triangulating between these readily identifiable bony landmarks and then refining the location with a ruler.

Surgical findings were recorded on the patient-specific acetabular projection. A modified Beck scale was used to characterize the degree of articular cartilage damage (3) (Table 2). Control ROIs were specifically assessed for clinical signs of cartilage damage. The surgeon of record performed all assessments, and, although he was provided with the clinical radiology report, he was blinded to the T2* mapping data.

Statistical Analysis

ROIs were assigned to four groups according to the Beck scale (1, 2, 3 and 4, and 5 and 6) (Table 2). Subsequently, the T2* values were compared among these groups by conducting pair-wise Wilcoxon rank sum tests (39). $P < .05$ was indicative of a significant difference. To ensure a family-wise error rate no larger than the significance level, we corrected the P values by using the method used by Holm (40). Finally, the groups were investigated with multiple dichotomizations to estimate a predictive model by using each of the resulting binary data sets. We then used ROC analysis to evaluate the sensitivity and specificity of our predictive models and to define a threshold T2* value for damaged articular cartilage. The threshold value was taken to be the value of T2* that corresponds to the point on the ROC curve at which the sensitivity is equal to 1 minus specificity.

Interobserver reliability was assessed by assigning two examiners of differing experience levels (C.Z. and M.B., with 1 year of experience) to independently generate ROIs and T2* values from five randomly selected hips. Each examiner made measurements from the same sagittal sections of blinded MR images. Subsequently, a single-measure interclass correlation coefficient was used to determine within-ROI variability between groups.

Assessment of the variation in the T2* data owing to the orientation with respect to the main magnetic field (B_0)—the magic angle effect—was done by fitting a linear regression model with T2* values as the response and $3\cos^2\{[(x - 15)\pi]/180\} - 1$ as the predictor, where x is the angle in degrees (41). A fixed angle of 15° was used to correct for the average orientation of the 12-o'clock line that was used in the calculation of the ROI angles.

All statistical analyses were performed by a biostatistician (J.H., with 7 years of experience) with use of the R software package (version 2.15.2; R: A language and environment for statistical computing, R core Team 2012R, Foundation for Statistical Computing, Vienna, Austria).

Results

Patients and Clinical Assessment

Twenty-six patients with 28 consecutive hip MR examinations met the inclusion criteria. There were 18 female and eight male patients. The mean age of all patients was 28.2 years (range, 12–53 years), the mean age of male patients (nine hips) was 26.7 years (range, 16–53 years), and the mean age of female patients (19 hips) was 28.9 years (range, 12–46 years). Patients presented with characteristic symptoms of FAI, including groin pain, sitting intolerance, and limited hip range of motion. An average of 3 months elapsed between MR imaging and arthroscopy. Radiographic evaluation revealed an average α angle (±standard deviation) of 62.6° ± 14.5 and an average lateral center edge angle of 28.9° ± 6 (Fig 4). Tönnis grading revealed nine hips with Tönnis grade 0 and 19 hips with Tönnis grade 1 joint space.

MR Imaging and Image Processing

Fifty-seven ROIs were studied per patient, for a total of 532 full-thickness ROIs. These ROIs were further split into superficial and deep halves, resulting in 1596 ROIs overall. The results of quantitative T2* relaxation time mapping for the deep, superficial, and full-thickness acetabular cartilage layers are summarized in Table 3.

Arthroscopy

One hundred seventy-two of the 532 full-thickness ROIs (32%) were classified as Beck 1 (normal, macroscopically sound articular cartilage) at arthroscopy. One hundred sixty of the 532 ROIs (30%) showed cartilage changes of softening and fibrillation and were classified as Beck 2. One hundred seventy-one of the 532 ROIs (32%) were found to have either cartilage debonding (Fig 5) or gross delamination consistent with cleavage (Fig 6, *A*), with 112 (21%) classified as Beck 3 changes and 59 (11%) as Beck 4 changes. Twenty-one of the 532 ROIs (4%) had a fibrinous base (Beck 5) and eight (2%) had an eburnated base (Beck 6) denuded of

Figure 4

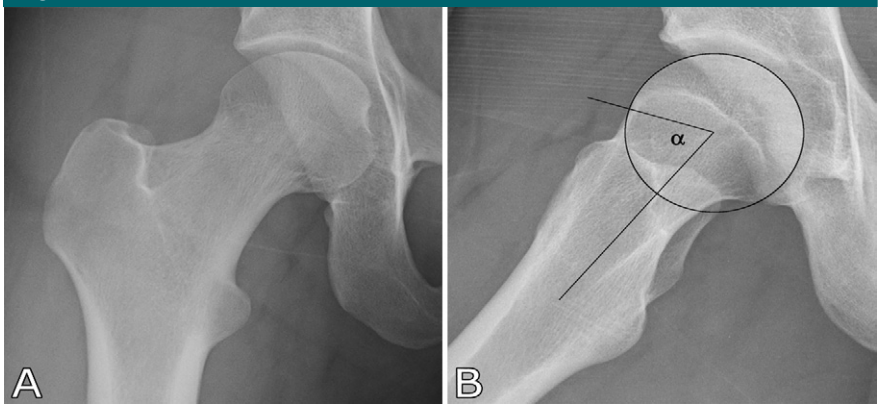

Figure 4: Representative clinical radiographs obtained in, *A*, anteroposterior and, *B*, frog leg lateral views. Anteroposterior radiograph reveals a reduced femoral head-neck offset, which is measured on frog leg lateral view. The α angle is 65°, which can be seen in clinical context of cam-type impingement indicative of a reduced femoral head-neck offset. Joint spaces are preserved on both radiographs.

Table 3

Average T2* Values in All Analyzed ROIs according to Modified Beck Scale

Layer	Beck Score 1	Beck Score 2	Beck Scores 3 and 4	Beck Scores 5 and 6
Full cartilage thickness	35.3 ± 7.0	20.7 ± 6.0	19.8 ± 5.6	16.8 ± 4.0
Superficial cartilage	40.1 ± 10.3	24.2 ± 7.4	22.5 ± 6.8	17.7 ± 5.0
Deep cartilage	30.6 ± 6.5	17.4 ± 5.5	17.2 ± 5.1	15.8 ± 4.0

Note.—Data are in milliseconds. Beck score 1 (normal) was statistically different from all other scores ($P < .001$) for full thickness, superficial, and deep cartilage; there was no significant difference among Beck scores 2–6.

cartilage. The cartilage thickness was preserved in 503 of the 532 ROIs (95%) (Beck 1–4). Because we excluded patients with joint space narrowing (Tönnis grade 2 and higher), only a very limited number of ROIs (5%, 29 of 532 ROIs) exhibited altered thickness of cartilage. As exemplified in Figure 6, the area of acetabular cartilage delamination as depicted at arthroscopy (Fig 6, *A*) correlates with markedly decreased T2* values (Fig 6, *B*) on the quantitative MR imaging map, whereas the plain radiograph (Fig 6, *C*) reveals Tönnis grade 0 and 1 with a preserved joint space.

Statistical Analysis

Interobserver reliability for the generation of acetabular deep, superficial, and full-thickness ROIs was found to have an estimated intraclass correlation coefficient of 0.88 (95% confidence interval: 0.82, 0.92). Assessment of the magic angle effect in the articular cartilage showed that, at most, 2% of the variation in the T2* data was due to orientation with respect to the main magnetic field (B_0), as indicated by R^2 of 0.02 with the linear regression model.

In these patients with FAI, T2* maps were found to have significantly lower values in regions with surgically identified cartilage damage (mean, 20.7 msec ± 6.0) than for normal cartilage (mean, 35.3 msec ± 7.0) ($P < .001$) (Table 3). The T2* values in the superficial layer were consistently higher than those in the deep cartilage layer ($P < .001$). For full, superficial, and deep cartilage, there was a significant difference between Beck scores 1 and 2 as well as between Beck score 1 and Beck scores 3 and 4 ($P = < .001$ for both). The respective box plots for T2* values in the different Beck scale groups are

Figure 5

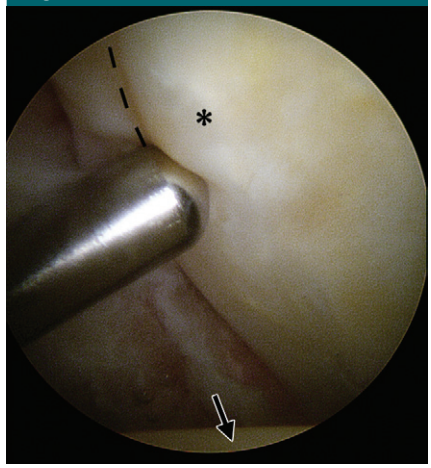

Figure 5: Arthroscopic view demonstrates appearance of cartilage debonding (*). Arrow indicates femoral head, and dashed line indicates chondrolabral junction. Note that area of debonding subjacent to chondrolabral junction can be displaced from undersurface without evidence of a tear reaching the surface, also called "carpet phenomenon" (Beck score = 3). Area of cartilage debonding appears whiter than surrounding areas.

demonstrated in Figure 7, *A*. The ROC curves indicated clear differentiation for all dichotomizations separating group 1 (normal) from all other Beck scale levels (Fig 7, *B* and *C*). At ROC analysis of higher grades (ie, Beck scores 3 and 4 vs Beck scores 5 and 6), no clear differentiation was observed (Fig 7, *D*). ROC curve analysis showed that a 91% true-positive and 13% false-positive rate corresponded with a threshold T2* value of 28 msec for defining cartilage damage, a value that corresponds to an estimated probability of disease of 0.8.

Note that all *P* values were corrected for multiple comparisons. The unadjusted *P* values were so small that adjusting for multiple comparisons did not affect the conclusions.

Discussion

Since its description and means of surgical correction were first published, the surgical management of FAI has become increasingly common (1,42). Significant variation, however, has been seen in surgical outcomes, an

Figure 6

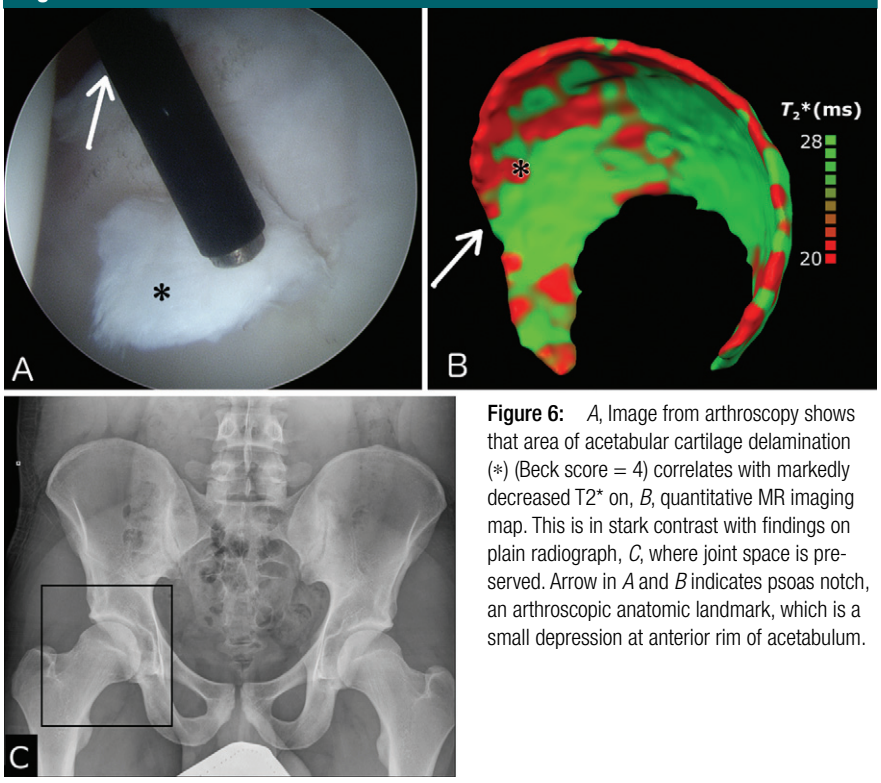

Figure 6: *A*, Image from arthroscopy shows that area of acetabular cartilage delamination (*) (Beck score = 4) correlates with markedly decreased T2* on, *B*, quantitative MR imaging map. This is in stark contrast with findings on plain radiograph, *C*, where joint space is preserved. Arrow in *A* and *B* indicates psoas notch, an arthroscopic anatomic landmark, which is a small depression at anterior rim of acetabulum.

issue that has been explained in part by the presence or absence of articular cartilage damage (9,11). Because of the abnormal contact stresses between the reduced femoral head-neck offset and the acetabulum, debonding occurs between the cartilage and subchondral bone plate. This "inside out" process of articular cartilage delamination progressing from deep to superficial is unique to FAI. Therefore, previous imaging and arthroscopic staging guidelines, such as the International Cartilage Repair Society classification (43), which was created to describe the degenerative changes in the knee from superficial to deep, are limited in their application for the hip.

Currently, radiographic Tönnis grading is the most commonly used means of screening for level of cartilage damage incompatible with joint preservation surgery (10,15). Tönnis grading, unfortunately, is unreliable (14,35). Our findings were consistent with this; despite the fact that we restricted surgery to patients with Tönnis grades 0 or 1, 360 of the 532 ROIs (68%) showed evidence of cartilage damage at arthroscopy. This underscores the relative insensitivity of radiography in determining the extent of osteoarthritis in this cohort.

Efforts to improve cartilage assessment with routine MR imaging have been disappointing (12,16–19). Cartilage debonding and gross delamination may appear normal at routine MR imaging and MR arthrography (17,44,45). The "inverted Oreo cookie sign" (46), which is seen when contrast material becomes interposed between debonded cartilage and bone, is specific but has low sensitivity (17). We question if this is a consequence of the hip's inherent congruency, which may prevent contrast material flow between delaminated cartilage and bone. The occurrence of a linear, dark line on T1-weighted images extending from the chondrolabral junction has also been noted. This line is of uncertain importance and may simply represent a truncation artifact (47). Low T1- and T2-weighted signal intensity has been observed in delaminated cartilage (17). Without the ability to be quantified, this observation has been of limited utility.

In our study, however, we report new MR imaging findings, confirmed with arthroscopy, that may have substantial clinical diagnostic implications. Namely, we found a significant correlation between cartilage damage and decreased T2* values. This is consistent with findings from previous reports (31–34,48). ROC curve analysis showed that a 91% true-positive and 13% false-positive rate corresponded with a threshold T2* value of 28 msec at 3.0 T for defining cartilage damage, a value that corresponds to an estimated probability of disease of 0.8. We believe that this threshold will be helpful for clinicians interpreting the results of T2* maps and may provide the basis for an MR imaging–guided cartilage screening tool similar to, but more reliable than, Tönnis grading.

T2 relaxation time has been used as an indirect indicator of structural changes within articular cartilage owing to its sensitivity to alterations in water content (49), interaction between water molecules, and spatial collagen architecture (50,51). T2* relaxation is a combination of inherent "true" T2 relaxation and additional T2′ relaxation due to both microscopic and macroscopic magnetic field inhomogeneities ($1/T2^* = 1/T2 + 1/T2'$). The reversible relaxation due to these inhomogeneities can be refocused and thus removed by using a 180° pulse for measurement of T2. In gradient-recalled echo sequences, however, there is no such refocusing pulse and the additional relaxation effects characterized with the parameter T2′ are not removed. Thus, T2* is sensitive to T2 changes as well as to additional mechanisms that contribute to T2′. Although the latter component is affected by bulk inhomogeneities in the static magnetic field, which are typically not of interest, it is also affected by the differences in tissue composition at a microscopic level (52), such as changes at the osteochondral interface and the

Figure 7

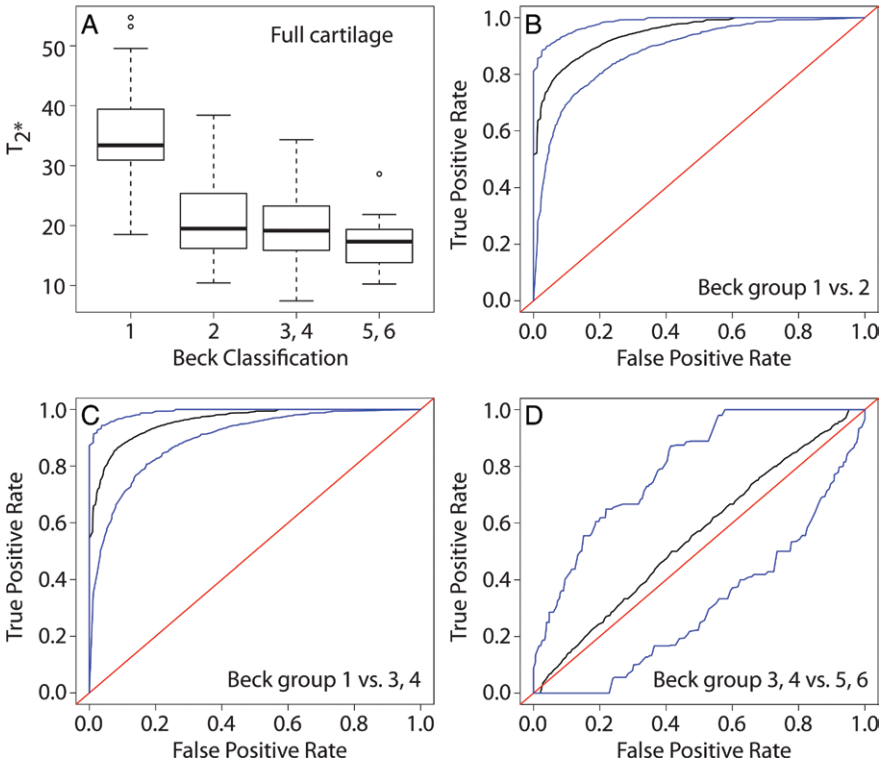

Figure 7: *A*, Box plots for T2* values according to modified Beck scale over all patients and ROIs. Box plots show minimum, median, and maximum values. ○ = outlier. *B*, ROC curve (black) and delineation of 95% confidence band of ROC curve (blue) for differentiating between Beck scores 1 and 2 with T2*. *C*, ROC curve (black) and delineation of 95% confidence band of ROC curve (blue) for differentiating Beck score 1 from Beck scores 3 and 4. Beck 1 cartilage was clearly differentiated from more diseased cartilage. *D*, ROC curve (black) and delineation of 95% confidence band of ROC curve (blue) for differentiating Beck score 3 and 4 cartilage from Beck score 5 and 6 cartilage show no differences between groups. Red line in ROC graphs indicates efficacy of random prediction.

susceptibility changes induced by para- and/or diamagnetic alterations within the cartilage matrix.

MR arthrography and histologic correlations in cadaveric specimens have revealed fibrocartilage transformation with superimposed deposition of calcium hydroxyapatite (53). Furthermore, fibrocartilagenous metaplasia undergoes mineralization by osteoblasts with penetration of capillaries at the osteochondral junction and subsequent deposition of osteoid matrix (54). This was also confirmed in small biopsies of symptomatic patients with FAI (55), clearly indicating the correlation of cartilage delamination in FAI with loss of normal hyaline cartilage architecture, which had been transformed into fibrous connective tissue. Granulation tissue with calcifications and osseous callus at its base was noted in reparative zones. Given these histologic findings, such microscopic inhomogeneities inherent to the disease process can increase the sensitivity of T2* relative to T2. The damaged acetabular cartilage consists mostly of fibrous metaplasia and fibrocartilage-like tissue lacking a highly organized collagen network, which is reflected by the loss of the zonal variation of T2 observed in native cartilage (56). Similar to previous accounts, microfracture repair sites with fibrocartilage-like repair tissue show lower mean T2 values than control cartilage after microfracture procedures (26,57,58). A lower T2 value may suggest overall loss of mobile water molecules and decreased mobility of the remaining water molecules within the milieu of randomly oriented fibrous tissue. The additional T2* effect due to the lack of a 180° refocusing pulse that would be applied in pure T2 mapping can arise from the calcium deposits, further decreasing the measured T2* relaxation time.

The T2* studies were conducted in addition to the regular clinical imaging examination with intraarticular gadolinium; as such, gadolinium was present during T2* mapping. Nieminen et al (59) have reported that the influence of gadolinium on cartilage T2 is insignificant, concluding that, in clinical trials involving gadolinium (delayed gadolinium-enhanced MR imaging of cartilage), T2 measurement could be done during the same imaging session unless very high doses are used. Our experimental T2* evidence is consistent with this. The T2* relaxation times of the weight-bearing acetabular cartilage of two patients were assessed with T2* maps, measured both with and without gadolinium during the same examination. The comparison between the data sets demonstrated near-perfect agreement, with an R^2 value of 0.97 between the pre- and postgadolinium T2* values, indicating that 97% of the variation in pregadolinium T2* is explained by the postgadolinium T2*. The average difference in the relaxation times was less than 1 msec (pregadolinium T2* = 19.6 msec, postgadolinium T2* = 20.3 msec [n = 129]; P = .1145, Wilcoxon test), further indicating that with the current (conventional clinical imaging) protocol, the influence of gadolinium on T2* relaxation time of acetabular cartilage is virtually nonexistent.

We also found that T2* mapping with its inherent high signal-to-noise ratio and resolution enables the division of hip cartilage into femoral and acetabular cartilage, consistent with previous reports (60,61). This is a significant advantage when imaging patients with FAI, a condition in which isolated acetabular cartilage damage is common (3,6). We further divided the acetabular ROIs into deep and superficial halves;

our finding of significantly different T2* values in the deep and superficial layers is in keeping with findings from previous reports (26).

The use of a clock face nomenclature to describe acetabular findings is common to both the radiology and orthopedic literature (3,45,62,63). It is important to note that these two uses are anatomically unrelated and cannot be directly compared. In the radiology literature, the 12-o'clock position is defined by the MR image and is the superior point on a sagittal section, which depends on the patient's lumbar lordosis and/or pelvic tilt. In the orthopedic literature, however, the 12-o'clock position is defined by anatomic landmarks and is the point on the acetabular rim directly above and centered on the acetabular notch. To our knowledge, the acetabular projection technique presented herein is the only technique that enables accurate comparison of imaging and surgical findings.

However, a limitation of our study remains that there is no validating test to assess how closely the ROIs drawn on the MR images match those on the arthroscopic images. There is also human error involved in drawing the ROIs, which we addressed by testing the interobserver reliability. Another limitation of the study is the two-dimensional multisection acquisition of the T2* data. Although this approach provides a high signal-to-noise ratio and good detail in the sections perpendicular to the cartilage, curvature of the acetabulum prevents reliable assessment of the cartilage in the border sections. Furthermore, the resolution of the T2* maps was 0.52 × 0.52 × 3 mm, interpolated to 0.26 × 0.26 × 3 mm; although this allowed good definition of the ROIs, the partial volume effect likely occurs—specifically when separating deep and superficial cartilage. It should also be noted that the absolute T2* relaxation times are affected by a number of factors, such as acquisition parameters, regional variations in the transmit radiofrequency (B_1) field, eddy currents, and the choice of fitting algorithm and fitting parameters. Therefore, caution should be exercised when interpreting and extrapolating the disease probability threshold T2* value of our study, which was derived from our patient data sets to other sites and data acquired on imaging units from other manufacturers. This represents a limitation, and further independent studies are needed. Finally, the relatively small number of patients and the lack of a histologic standard of reference limit the strength of our study.

In conclusion, our results indicate that T2* mapping can become a valuable diagnostic method for routine evaluation of acetabular cartilage in FAI with existing clinical MR units. The patient-specific acetabular projection allows for good anatomic localization of MR imaging data, facilitating preoperative evaluation and long-term cartilage monitoring.

Our study demonstrates the ability of quantitative T2* mapping to help accurately diagnose damaged acetabular cartilage in FAI. T2* mapping is a widely available clinical sequence with a high signal-to-noise ratio and resolution that does not require intravenous contrast material, making it a practical addition to routine clinical imaging. The patient-specific acetabular projection presented herein enables the clinician to easily assess where on the acetabulum damage has occurred. As a research tool, the combination of T2* data that detail damaged cartilage and a flattened acetabular projection that shows the location of the damage will allow a longitudinal study of the natural history of acetabular cartilage in patients with FAI.

Disclosures of Conflicts of Interest: J.E. Financial activities related to the present article: none to disclose. Financial activities not related to the present article: none to disclose. Other relationships: has a patent application pending. **C.Z.** No relevant conflicts of interest to disclose. **M.J.N.** Financial activities related to the present article: none to disclose. Financial activities not related to the present article: none to disclose. Other relationships: has a patent application pending. **R.G.** No relevant conflicts of interest to disclose. **J.H.** No relevant conflicts of interest to disclose. **M.B.** No relevant conflicts of interest to disclose. **P.H.** No relevant conflicts of interest to disclose. **P.M.** Financial activities related to the present article: none to disclose. Financial activities not related to the present article: none to disclose. Other relationships: has a patent application pending.

References

1. Ganz R, Parvizi J, Beck M, Leunig M, Nötzli H, Siebenrock KA. Femoroacetabular impingement: a cause for osteoarthritis of the hip. Clin Orthop Relat Res 2003;(417):112–120.
2. Leunig M, Beaulé PE, Ganz R. The concept of femoroacetabular impingement: current status and future perspectives. Clin Orthop Relat Res 2009;467(3):616–622.
3. Beck M, Kalhor M, Leunig M, Ganz R. Hip morphology influences the pattern of damage to the acetabular cartilage: femoroacetabular impingement as a cause of early osteoarthritis of the hip. J Bone Joint Surg Br 2005;87(7):1012–1018.
4. Dudda M, Albers C, Mamisch TC, Werlen S, Beck M. Do normal radiographs exclude asphericity of the femoral head-neck junction? Clin Orthop Relat Res 2009;467(3):651–659.
5. Allen D, Beaulé PE, Ramadan O, Doucette S. Prevalence of associated deformities and hip pain in patients with cam-type femoroacetabular impingement. J Bone Joint Surg Br 2009;91(5):589–594.
6. Ganz R, Leunig M, Leunig-Ganz K, Harris WH. The etiology of osteoarthritis of the hip: an integrated mechanical concept. Clin Orthop Relat Res 2008;466(2):264–272.
7. Philippon M, Schenker M, Briggs K, Kuppersmith D. Femoroacetabular impingement in 45 professional athletes: associated pathologies and return to sport following arthroscopic decompression. Knee Surg Sports Traumatol Arthrosc 2007;15(7):908–914.
8. Philippon MJ, Briggs KK, Yen YM, Kuppersmith DA. Outcomes following hip arthroscopy for femoroacetabular impingement with associated chondrolabral dysfunction: minimum two-year follow-up. J Bone Joint Surg Br 2009;91(1):16–23.
9. Beck M, Leunig M, Parvizi J, Boutier V, Wyss D, Ganz R. Anterior femoroacetabular impingement. II. Midterm results of surgical treatment. Clin Orthop Relat Res 2004;(418):67–73.
10. Larson CM, Giveans MR, Taylor M. Does arthroscopic FAI correction improve function with radiographic arthritis? Clin Orthop Relat Res 2011;469(6):1667–1676.
11. Guanche CA, Chan KA, Conner CA, Sikka RS. Paper 4: arthroscopic treatment cam-type hip impingement lesions with 32.8-month mean follow-up. Arthroscopy 2012;28(6 Suppl 2):e:45.
12. Byrd JW, Jones KS. Arthroscopic management of femoroacetabular impingement: minimum 2-year follow-up. Arthroscopy 2011;27(10):1379–1388.

13. Clohisy JC, Carlisle JC, Trousdale R, et al. Radiographic evaluation of the hip has limited reliability. Clin Orthop Relat Res 2009;467(3):666–675.

14. Carlisle JC, Zebala LP, Shia DS, et al. Reliability of various observers in determining common radiographic parameters of adult hip structural anatomy. Iowa Orthop J 2011;31:52–58.

15. Tönnis D. Congenital dysplasia and dislocation of the hip in children and adults. Berlin, Germany: Springer, 1987.

16. Anderson LA, Peters CL, Park BB, Stoddard GJ, Erickson JA, Crim JR. Acetabular cartilage delamination in femoroacetabular impingement: risk factors and magnetic resonance imaging diagnosis. J Bone Joint Surg Am 2009;91(2):305–313.

17. Pfirrmann CW, Duc SR, Zanetti M, Dora C, Hodler J. MR arthrography of acetabular cartilage delamination in femoroacetabular cam impingement. Radiology 2008;249(1):236–241.

18. Blankenbaker DG, Ullrick SR, Kijowski R, et al. MR arthrography of the hip: comparison of IDEAL-SPGR volume sequence to standard MR sequences in the detection and grading of cartilage lesions. Radiology 2011;261(3):863–871.

19. Gold SL, Burge AJ, Potter HG. MRI of hip cartilage: joint morphology, structure, and composition. Clin Orthop Relat Res 2012;470(12):3321–3331.

20. Zlatkin MB, Pevsner D, Sanders TG, Hancock CR, Ceballos CE, Herrera MF. Acetabular labral tears and cartilage lesions of the hip: indirect MR arthrographic correlation with arthroscopy—a preliminary study. AJR Am J Roentgenol 2010;194(3):709–714.

21. Pfirrmann CW, Mengiardi B, Dora C, Kalberer F, Zanetti M, Hodler J. Cam and pincer femoroacetabular impingement: characteristic MR arthrographic findings in 50 patients. Radiology 2006;240(3):778–785.

22. Kim YJ, Jaramillo D, Millis MB, Gray ML, Burstein D. Assessment of early osteoarthritis in hip dysplasia with delayed gadolinium-enhanced magnetic resonance imaging of cartilage. J Bone Joint Surg Am 2003;85-A(10):1987–1992.

23. Mamisch TC, Kain MS, Bittersohl B, et al. Delayed gadolinium-enhanced magnetic resonance imaging of cartilage (dGEMRIC) in femoacetabular impingement. J Orthop Res 2011;29(9):1305–1311.

24. Zilkens C, Holstein A, Bittersohl B, et al. Delayed gadolinium-enhanced magnetic resonance imaging of cartilage in the long-term follow-up after Perthes disease. J Pediatr Orthop 2010;30(2):147–153.

25. Lattanzi R, Petchprapa C, Glaser C, et al. A new method to analyze dGEMRIC measurements in femoroacetabular impingement: preliminary validation against arthroscopic findings. Osteoarthritis Cartilage 2012; 20(10):1127–1133.

26. Watanabe ABC, Boesch C, Siebenrock K, Obata T, Anderson SE. T2 mapping of hip articular cartilage in healthy volunteers at 3T: a study of topographic variation. J Magn Reson Imaging 2007;26(1):165–171.

27. Nishii T, Tanaka H, Sugano N, Sakai T, Hananouchi T, Yoshikawa H. Evaluation of cartilage matrix disorders by T2 relaxation time in patients with hip dysplasia. Osteoarthritis Cartilage 2008;16(2):227–233.

28. Nishii T, Shiomi T, Tanaka H, Yamazaki Y, Murase K, Sugano N. Loaded cartilage T2 mapping in patients with hip dysplasia. Radiology 2010;256(3):955–965.

29. Mosher TJ, Dardzinski BJ. Cartilage MRI T2 relaxation time mapping: overview and applications. Semin Musculoskelet Radiol 2004;8(4):355–368.

30. Gold GE, Chen CA, Koo S, Hargreaves BA, Bangerter NK. Recent advances in MRI of articular cartilage. AJR Am J Roentgenol 2009; 193(3):628–638.

31. Bittersohl B, Hosalkar HS, Hughes T, et al. Feasibility of T2* mapping for the evaluation of hip joint cartilage at 1.5T using a three-dimensional (3D), gradient-echo (GRE) sequence: a prospective study. Magn Reson Med 2009;62(4):896–901.

32. Bittersohl B, Miese FR, Hosalkar HS, et al. T2* mapping of hip joint cartilage in various histological grades of degeneration. Osteoarthritis Cartilage 2012;20(7):653–660.

33. Bittersohl B, Miese FR, Hosalkar HS, et al. T2* mapping of acetabular and femoral hip joint cartilage at 3 T: a prospective controlled study. Invest Radiol 2012;47(7):392–397.

34. Apprich S, Mamisch TC, Welsch GH, et al. Evaluation of articular cartilage in patients with femoroacetabular impingement (FAI) using T2* mapping at different time points at 3.0 Tesla MRI: a feasibility study. Skeletal Radiol 2012;41(8):987–995.

35. Clohisy JC, Carlisle JC, Beaulé PE, et al. A systematic approach to the plain radiographic evaluation of the young adult hip. J Bone Joint Surg Am 2008;90(Suppl 4):47–66.

36. Larson CM, Giveans MR, Stone RM. Arthroscopic débridement versus refixation of the acetabular labrum associated with femoroacetabular impingement: mean 3.5-year follow-up. Am J Sports Med 2012;40(5):1015–1021.

37. Rosset A, Spadola L, Ratib O. OsiriX: an open-source software for navigating in multidimensional DICOM images. J Digit Imaging 2004;17(3):205–216.

38. Goebel R. BrainVoyager: past, present, future. Neuroimage 2012;62(2):748–756.

39. Mann HB, Whitney DR. On a test of whether one of two random variables is stochastically larger than the other. Ann Math Stat 1947;18(1):50–60.

40. Holm S. A simple sequentially rejective multiple test procedure. Scand J Stat 1979;6(2):65–70.

41. Xia Y, Moody JB, Burton-Wurster N, Lust G. Quantitative in situ correlation between microscopic MRI and polarized light microscopy studies of articular cartilage. Osteoarthritis Cartilage 2001;9(5):393–406.

42. Ganz R, Gill TJ, Gautier E, Ganz K, Krügel N, Berlemann U. Surgical dislocation of the adult hip: a technique with full access to the femoral head and acetabulum without the risk of avascular necrosis. J Bone Joint Surg Br 2001;83(8):1119–1124.

43. Brittberg M. ICRS cartilage evaluation package. http://www.cartilage.org/_files/contentmanagement/ICRS_evaluation.pdf. Published 2000. Accessed August 6, 2002.

44. Mamisch TC, Zilkens C, Siebenrock KA, Bittersohl B, Kim YJ, Werlen S. MRI of hip osteoarthritis and implications for surgery. Magn Reson Imaging Clin N Am 2010;18(1):111–120.

45. Schmid MR, Nötzli HP, Zanetti M, Wyss TF, Hodler J. Cartilage lesions in the hip: diagnostic effectiveness of MR arthrography. Radiology 2003;226(2):382–386.

46. Beaulé PE, Zaragoza EJ. Surgical images: musculoskeletal acetabular cartilage delamination demonstrated by magnetic resonance arthrography: inverted "Oreo" cookie sign. Can J Surg 2003;46(6):463–464.

47. Frank LR, Brossmann J, Buxton RB, Resnick D. MR imaging truncation artifacts can create a false laminar appearance in cartilage. AJR Am J Roentgenol 1997;168(2):547–554.

48. Miese FR, Zilkens C, Holstein A, et al. Assessment of early cartilage degeneration after slipped capital femoral epiphysis using T2 and T2* mapping. Acta Radiol 2011;52(1):106–110.

49. Liess C, Lüsse S, Karger N, Heller M, Glüer CC. Detection of changes in cartilage water content using MRI T2-mapping in vivo.

Osteoarthritis Cartilage 2002;10(12):907–913.

50. Nieminen MT, Rieppo J, Töyräs J, et al. T2 relaxation reveals spatial collagen architecture in articular cartilage: a comparative quantitative MRI and polarized light microscopic study. Magn Reson Med 2001;46(3):487–493.
51. Burstein D, Gray M, Mosher T, Dardzinski B. Measures of molecular composition and structure in osteoarthritis. Radiol Clin North Am 2009;47(4):675–686.
52. Chavhan GB, Babyn PS, Thomas B, Shroff MM, Haacke EM. Principles, techniques, and applications of T2*-based MR imaging and its special applications. RadioGraphics 2009;29(5):1433–1449.
53. Sampatchalit S, Chen L, Haghighi P, Trudell D, Resnick DL. Changes in the acetabular fossa of the hip: MR arthrographic findings correlated with anatomic and histologic analysis using cadaveric specimens. AJR Am J Roentgenol 2009;193(2):W127–W133.
54. Noguchi Y, Miura H, Takasugi S, Iwamoto Y. Cartilage and labrum degeneration in the dysplastic hip generally originates in the anterosuperior weight-bearing area: an arthroscopic observation. Arthroscopy 1999;15(5):496–506.
55. Kohl S, Hosalkar HS, Mainil-Varlet P, Krueger A, Buechler L, Siebenrock K. Histology of damaged acetabular cartilage in symptomatic femoroacetabular impingement: an observational analysis. Hip Int 2011;21(2):154–162.
56. Watanabe A, Boesch C, Anderson SE, Brehm W, Mainil Varlet P. Ability of dGEMRIC and T2 mapping to evaluate cartilage repair after microfracture: a goat study. Osteoarthritis Cartilage 2009;17(10):1341–1349.
57. Welsch GH, Mamisch TC, Domayer SE, et al. Cartilage T2 assessment at 3-T MR imaging: in vivo differentiation of normal hyaline cartilage from reparative tissue after two cartilage repair procedures—initial experience. Radiology 2008;247(1):154–161.
58. Oneto JM, Ellermann J, LaPrade RF. Longitudinal evaluation of cartilage repair tissue after microfracture using T2-mapping: a case report with arthroscopic and MRI correlation. Knee Surg Sports Traumatol Arthrosc 2010;18(11):1545–1550.
59. Nieminen MT, Menezes NM, Williams A, Burstein D. T2 of articular cartilage in the presence of Gd-DTPA^{2-}. Magn Reson Med 2004;51(6):1147–1152.
60. Li W, Abram F, Beaudoin G, Berthiaume MJ, Pelletier JP, Martel-Pelletier J. Human hip joint cartilage: MRI quantitative thickness and volume measurements discriminating acetabulum and femoral head. IEEE Trans Biomed Eng 2008;55(12):2731–2740.
61. Zilkens C, Miese F, Kim YJ, et al. Three-dimensional delayed gadolinium-enhanced magnetic resonance imaging of hip joint cartilage at 3T: a prospective controlled study. Eur J Radiol 2012;81(11):3420–3425.
62. Wall PD, Hossain M, Ganapathi M, Andrew JG. Sexual activity and total hip arthroplasty: a survey of patients' and surgeons' perspectives. Hip Int 2011;21(2):199–205.
63. Studler U, Kalberer F, Leunig M, et al. MR arthrography of the hip: differentiation between an anterior sublabral recess as a normal variant and a labral tear. Radiology 2008;249(3):947–954.